A Study on Thermal Loading Effects in Tankers

Tae-Min Cho <tm1.cho@samsung.com >, Bong-Jae Kim <bj72.kim@samsung.com>,
Ki-Bok Jang <kibok.jang@samsung.com>, Yong-Suk Suh <yongsuk.suh@samsung.com>

Marine Research Institute, Samsung Heavy Industries Co., Ltd., Korea

Abstract

In this study, strength analysis of cargo hold by considering thermal loading is performed through finite element analysis. In general, tankers are designed by CSR (Common Structural Rules for Double Hull Oil Tankers) and various combinations of mechanical loading are considered in CSR. CSR is based on design temperatures for the cargoes up to 80℃. Since thermal loading is considered as tertiary load in CSR, deformation loads caused by thermal loading is not covered in CSR and so far there have been few studies on the design of cargo hold considering thermal loading. In this study, the strength analysis of a cargo hold is performed considering thermal loading, mechanical loading, and combination of thermal and mechanical loading. Through analysis, the effect of thermal loading on stress distribution and buckling is observed. In the design of the cargo hold it may be necessary to consider the effects of thermal loading and further studies are required in the relevant industries.

1 Introduction

In general, tankers are designed by CSR (Common Structural Rules for Double Hull Oil Tankers) [1]. In CSR, various combinations of mechanical loading are considered. CSR is based on design cargo temperatures between a minimum and maximum cargo temperature of 0℃ and 80℃ (3.1.8.4 of CSR). Since thermal loading is considered as a tertiary load in CSR, deformation loads caused by thermal loading are not covered. So far, there have been many studies on the design of tankers and cargo holds [2-7], however few studies have considering thermal loading.
In this study, strength analysis of a cargo hold considering thermal loading a heated cargo is performed through finite element analysis. Thermal loading, mechanical loading, and the combined loading are applied to the cargo hold. Through the analyses, the effect of thermal loading on stress distribution and buckling is investigated. This paper is composed of five sections. In Section 2, cargo hold model and loading conditions are explained. In Section 3, the temperature distribution of the cargo hold is presented. In Section 4, the strength analysis of cargo hold by considering thermal loading is performed and the results are discussed. Finally, conclusions are drawn in Section 5.

2 Cargo hold model

The cargo hold model and the coordinate system used in this study are shown in Fig. 1. The principal dimensions of cargo hold are 100m×50m×25m (L×B×H). The cargo hold is divided into three sections - AFT, Middle, and FWD section. Longitudinal and transverse plates (such as deck, bottom transverse bulkhead, vertical web, etc.) are represented by shell elements. Longitudinal and transverse stiffeners and face plates of vertical webs are represented by bar elements with bending stiffness. The reduced thickness used in the FE model of the cargo holds, applicable to all plating and stiffener’s web and flanges is to be calculated as follows,

$$t_{FEM\text{-}net50} = t_{grs} - 0.5t_{corr}$$

Where

t_{grs} gross thickness

t_{corr} corrosion addition, as defined in CSR (Table 6.3.1 and Figure 6.3.1)

Mechanical material properties are shown in Table 1. The reference temperature for thermal expansion is 15 ^{o}C. In this study, the mechanical loading patterns are selected according to CSR (Table B.2.4). There are various mechanical loading patterns in CSR. Among them, the thermal loading patterns are selected as shown in Fig. 2 and Table 2. For each thermal loading pattern, 50 ℃ and 80 ℃ of cargo temperature are considered as shown in Table 3. In Table 3, temperatures of air and sea water are reasonably assumed.

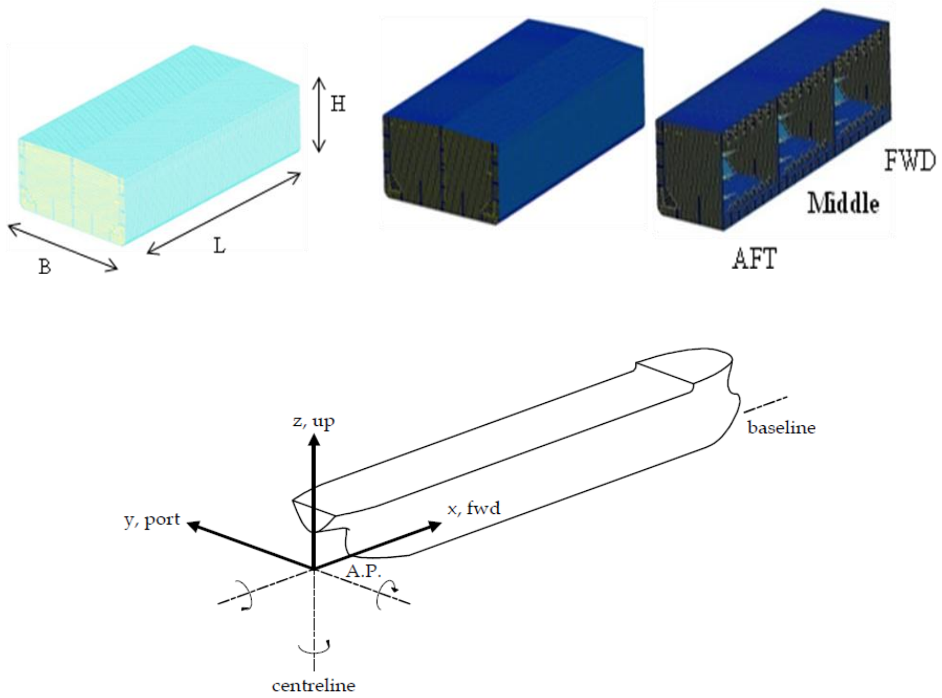

Fig. 1 Cargo hold model and coordinate system

Table 1 Mechanical material property

Material	Young's modulus (MPa)	Poisson's ratio	Yield strength (MPa)	Thermal expansion coefficient (1/K)
Mild steel	206,000	0.3	235	1.2×10^{-5}
AH32	206,000	0.3	315	1.2×10^{-5}
AH36	206,000	0.3	355	1.2×10^{-5}

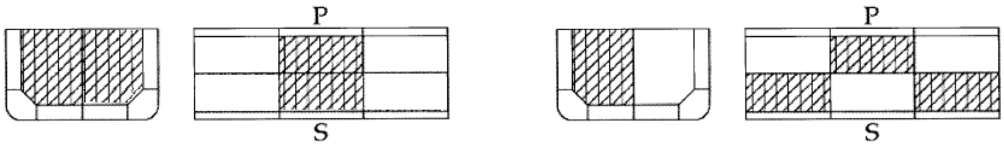

(a) Case A : symmetrical loading　　　(b) Case B : unsymmetrical loading

Fig. 2 Thermal loading pattern

Table 2 Load cases for cargo hold (Table B.2.4 of CSR)

Table B.2.4 Load Cases for Tankers with One Centreline Oil-tight Longitudinal Bulkhead							
Loading Pattern	Figure	Still Water Loads			Dynamic load cases		
		Draught	% of Perm. SWBM(2)	% of Perm. SWSF(2)	Strength assessment (1a)	Strength assessment against hull girder shear loads (1b)	
					Midship region	Forward region	Midship and aft regions
Design load combination S + D (Sea-going load cases)							
B1		$0.9\,T_{sc}$	100% (sag)	See note 3	1	\	\
			100% (hog)	100% (-ve fwd) See note 4	2, 5a	\	\
B2 (6)		$0.9\,T_{sc}$	100% (sag)	See note 3	1	\	\
			100% (hog)	100% (-ve fwd) See note 4	2, 5b	\	\
B3		$0.9\,T_{sc}$	100% (hog)	100% (-ve fwd) See note 5	2	4	2
				100% (-ve fwd) See note 4	5a, 5b, 6a, 6b	\	\
B4 Case B		$0.6\,T_{sc}$	100% (sag)	75% (+ve fwd) See note 4	1, 5a	\	\
B5 (6)		$0.6\,T_{sc}$	100% (sag)	75% (+ve fwd) See note 4	1, 5b	\	\
B6 Case A		$0.6\,T_{sc}$	100% (sag)	100% (+ve fwd) See note 5	1	3	1
				100% (+ve fwd) See note 4	5a, 5b	\	\

Table 3 Load cases and cargo temperature

Sub case	Wind speed	Temperature(℃)		
		Air	Sea water	Cargo
1	0 m/sec	5	2	50
2	0 m/sec	5	2	80

The mechanical boundary conditions are in accordance with coordinate system defined in Fig. 1. The mechanical boundary conditions to be applied at the ends of the cargo hold model are selected according to CSR (Table B.2.9) as shown in Table 4. Ground spring elements, i.e. spring elements with one end constrained in all 6 degrees of freedom, with stiffness in global y, z degree of freedom are applied to the grid points along deck, inner bottom, bottom shell and the vertical part of the side shells, inner hull longitudinal bulkheads, oil-tight longitudinal bulkheads as shown in Table 4 and Fig. 3 (Figure B.2.13 of CSR). The calculation of spring stiffness is defined in CSR (2.6.2). The thermal boundary conditions are explained in Section 3.

Table 4 Mechanical boundary conditions at model ends (Table B.2.9 of CSR)

Table B.2.9
Boundary Constraints at Model Ends

Location	**Translation**			**Rotation**		
	δ_x	δ_y	δ_z	θ_x	θ_y	θ_z
Aft End						
Aft end (all longitudinal elements)	***RL***	-	-	-	***RL***	***RL***
Independent Point aft end, see *Figure B.2.13*	Fix	-	-	-	$M_{v\text{-}end}$	$M_{h\text{-}end}$
Deck, inner bottom and outer shell	-	Springs	-	-	-	-
Side, inner skin and longitudinal bulkheads	-	-	Springs	-	-	-
Fore End						
Fore end (all longitudinal elements)	***RL***	-	-	-	***RL***	***RL***
Independent point fore end, see *Figure B.2.13*	-	-	-	-	$M_{v\text{-}end}$	$M_{h\text{-}end}$
Deck, inner bottom and outer shell	-	Springs	-	-	-	-
Side, inner skin and longitudinal bulkheads	-	-	Springs	-	-	-

Where:

- no constraint applied (free)

RL nodal points of all longitudinal elements rigidly linked to independent point at neutral axis on centreline

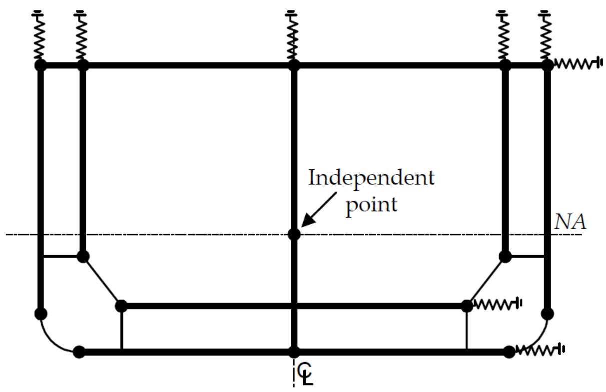

Fig. 3 Spring constraints ad model ends (Figure B.2.13 of CSR)

3 Temperature distribution of cargo hold

All temperatures (cargo, air, sea water) are assumed constant. The cargo is heated to maintain the temperature. Fig. 4 shows the schematic diagram of heat flux from outside to inside of tank.

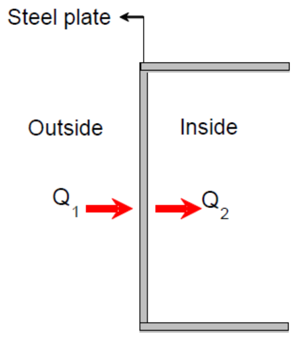

Fig. 4 Schematic diagram of heat flux from outside to inside of tank

Heat is normally transferred by three types of physical phenomena such as convection, conduction and radiation. These phenomena can be represented by numerical formulas. Heat fluxes across tank structure boundary shown in Fig. 4 can be expressed as Eq. (1).

$$Q_1 = U_1 A(T_1 - T_{steel}), \qquad Q_2 = U_2 A(T_{steel} - T_2) \tag{1}$$

Where,

U_1, U_2 : Overall heat transfer coefficients at each boundary
T_1, T_2 : Space temperatures (air, oil, compartment)
A : Surface area of steel plate

The temperature of the steel plate due to heat exchange with boundary conditions can be determined as Eq. (2) with the assumption of heat equilibrium state.

$$Q_1 = Q_2 = U_1 A(T_1 - T_{steel}) = U_2 A(T_{steel} - T_2)$$

$$T_{steel} = \frac{U_1 T_1 + U_2 T_2}{U_1 + U_2} \tag{2}$$

Generally, the overall heat transfer coefficients can be obtained as Eq. (3).

$$\frac{1}{U} = \frac{1}{(h_{1c} + h_{1r})} + \frac{e}{k} + \frac{1}{(h_{2c} + h_{2r})} \tag{3}$$

Where,

h_c : Convective heat transfer coefficient
h_r : Radiative heat transfer coefficient
k : Thermal conductivity of material
e : Thickness of material

At each boundary condition, the overall heat transfer coefficients can be applied as Eq. (4) and (5).

Tank surface exposed to external surrounding : $\dfrac{1}{U} = \dfrac{1}{(h_c + h_r)} + \dfrac{e_{steel}}{k_{steel}}$ (4)

Tank surface exposed to compartment : $\dfrac{1}{U} = \dfrac{1}{(h_c + h_r)}$ (5)

Heat transfer coefficients can be estimated by correlation equations through Yard's procedures. Thermal material properties at room temperature are listed in Table 5. Fig. 5 and 6 shows the temperature distribution of loading case A, when the cargo temperature is 50 °C and 80 °C, respectively. Since the thermal loading pattern is symmetric, so the temperature distribution is also symmetric. Fig. 7 and 8 shows the temperature distribution of loading case B, when the cargo temperature is 50 °C and 80 °C, respectively. As expected, the temperature distribution is unsymmetric due to the unsymmetrical loading pattern. These obtained temperature distributions are utilized as the input data of thermal loading.

Table 5 Thermal material property

	Thermal conductivity (W/K)	Kinematic viscosity (m^2/s)	Prandtl number
Mild steel, AH32, AH36	45.3	-	-
Air	0.0259	1.580×10^{-5}	0.724
Water	0.5610	8.012×10^{-7}	13.44
Oil	0.1068	1.787×10^{-6}	6.229

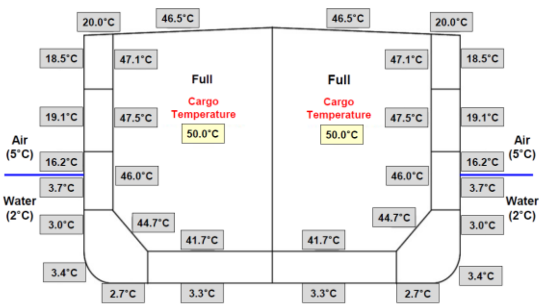

Fig. 5 Temperature distribution
(loading case A, cargo temperature : 50 °C)

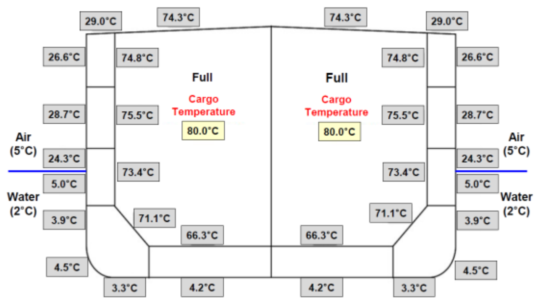

Fig. 6 Temperature distribution
(loading case A, cargo temperature : 80 °C)

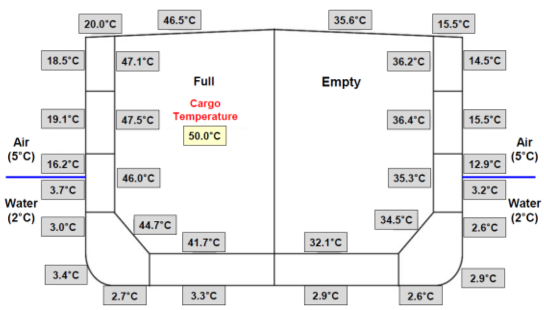

Fig. 7 Temperature distribution
(loading case B, cargo temperature : 50 °C)

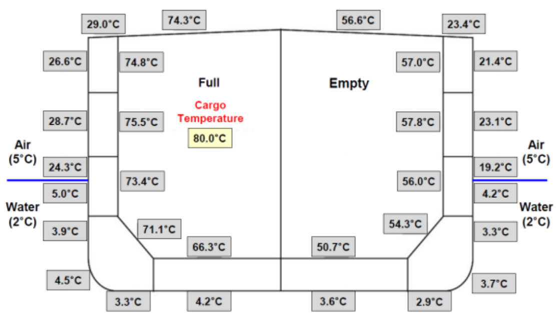

Fig. 8 Temperature distribution
(loading case B, cargo temperature : 80 °C)

4 Strength analysis of cargo hold

4.1 Stress distribution

Strength analysis of the cargo hold was performed by considering thermal loading only, mechanical loading only, and the combination of thermal and mechanical loading through MSC.NASTRAN 2010 [8]. The temperature distributions shown in Section 3 were used in calculation of the thermal stresses. The three-hold model shown in Fig. 1 was used in the finite element analysis, and the middle hold was only selected for the post-processing in order to get rid of any unfavorable boundary effects. The maximum von-Mises stress of each loading case is summarized in Table 6. These results were obtained through full finite element analysis. When the thermal loading is only applied, for all cases, the maximum von-Mises stress is lower than the yield strength. When the combined loading is applied, the maximum von-Mises stress is lower than the yield strength for 50 ^{o}C of cargo temperature. For 80^{o}C of cargo temperature, however, the maximum von-Mises stress is estimated about 13.6% and 6.3% greater than the yield strength in the mild steel region and AH32 region, respectively.

Table 6 Maximum von-Mises stress of cargo hold

Cargo temperature (^{o}C)	Loading case	Material	von-Mises stress(MPa)			Yield strength (MPa)	Overload
			Thermal loading	Mechanical loading	Combined loading		
50	A	Mild steel	131.0	183.0	225.0	235.0	
		AH32	89.4	302.0	315.0	315.0	
		AH36	106.0	333.0	346.0	355.0	
	B	Mild steel	121.0	179.0	221.0	235.0	
		AH32	88.0	251.0	280.0	315.0	
		AH36	105.0	312.0	317.0	355.0	
80	A	Mild steel	196.0	218.0	266.0	235.0	+13.6%
		AH32	149.0	302.0	335.0	315.0	+6.3%
		AH36	171.0	333.0	356.0	355.0	+0.0%
	B	Mild steel	195.0	179.0	265.0	235.0	+12.8%
		AH32	146.0	251.0	317.0	315.0	+1.0%
		AH36	115.0	312.0	321.0	355.0	

Fig. 9 shows von-Mises stress distribution of loading case A with 80 ^{o}C of cargo temperature at AFT T.BHD when the thermal loading is only applied. The maximum stress occurs in the top corner of AFT T.BHD. von-Mises stress at this point is 216MPa. Fig. 10 shows von-Mises distribution of loading case A with 80 ^{o}C of cargo temperature at AFT T.BHD when the combined loading is applied. von-Mises stress of top corner of AFT T.BHD is 211MPa. It is seen that stress distribution due to the thermal loading only is unrealistic and stress from the combined loading is not increased dramatically from that of the mechanical loading.

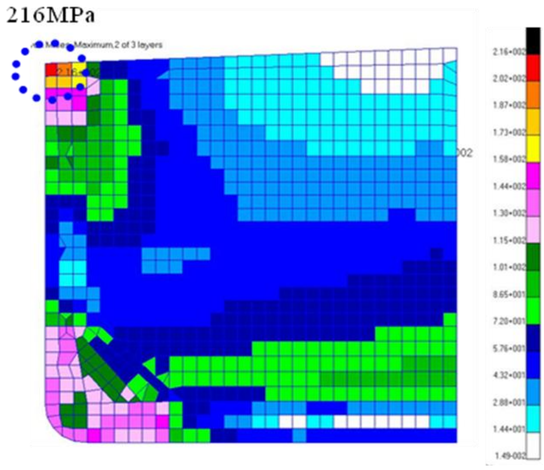

Fig. 9 von-Mises stress distribution of thermal loading only at AFT T.BHD

(loading case A, cargo temperature : 80 ^{o}C)

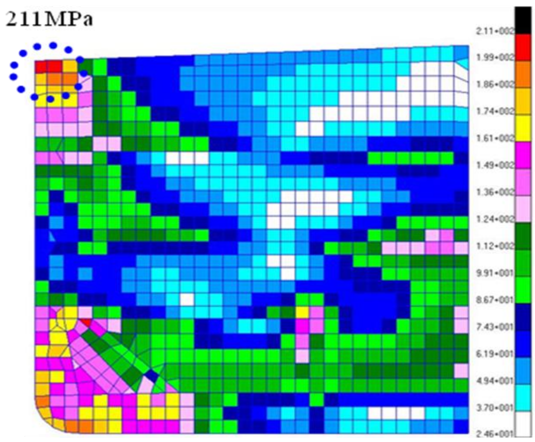

Fig. 10 von-Mises stress distribution of combined loading at AFT T.BHD

(loading case A, cargo temperature : 80 ^{o}C)

4.2 Buckling

In this section, the buckling factors are checked for the combined loading condition. Fig. 11 shows checked buckling regions. Table 7 shows the estimated buckling factor for the combined loading condition. In Table 7 the estimated buckling factors at T.BHD is greater than 1.0. Through the analyses, the effect of thermal loading on stress distribution and buckling is observed.

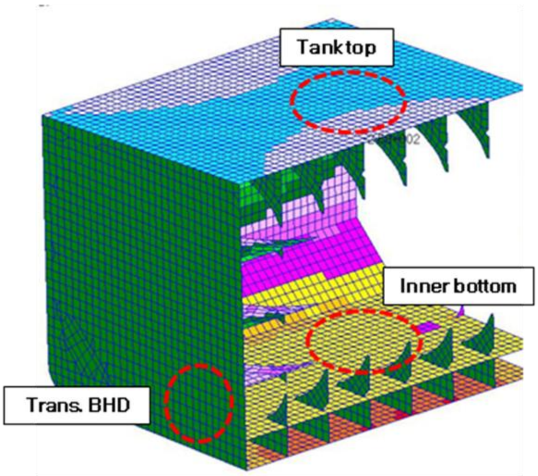

Fig. 11 Checked buckling regions

Table 7 Estimated buckling factors (combined loading)

ABS BUCKLING CALCULATION

- pr =	0.6	
- C1 =	1.1	
- C2 =	1.2	
- poiss' =	0.3	
- E =	2100000	kgf/cm²

- fcL_x : Crtical buckling stress for Long plate
- fcL_y : Crtical buckling stress for Wide plate
- fcL_z : Crtical buckling stress for Edge shear
- fy, fyi, fei,fcL : kgf/cm²
- σx = Actual compressive stress for Long plate, N/mm²
- σy = Actual compressive stress for Wide plate, N/mm²
- τ = Actual in-plane shear strss, N/mm²

Note:
1. Zero stress represent tensional stress
2. ID-1 means buckling result after stiffening

ID	fy / fyi	fyi_z / tn (cm)	s (cm) / l (cm)	ki_x / l/s	ki_y / ki_z	(fei)x / (fei)y	(fei)z	fcL_x / fcL_y	fcL_z	σx / σy	τ	factor
CaseA 50°C												
Tank Top plane	3211	1854	81.50	4.4	1.2849	4776	6542.1	2692.9	1727.8	237.00	10.00	0.91
	3211	1.950	437.00	5.36	6.027	1394.7		1394.7		16.10		
Inner bottom	2400	1386	81.50	4.4	1.2845	4183	5729.5	2069.5	1305.2	1.40	2.50	0.68
	2400	1.825	438.00	5.37	6.026	1221.3		1221.3		81.90		
T. BHD	2400	1386	81.50	4.4	1.2676	2986	4069.9	1937.1	1272.4	19.61	14.21	1.11
	2400	1.542	489.00	6.00	5.996	860.4		860.4		92.46		
CaseA 80°C												
ID	fy / fyi	fyi_z / tn (cm)	s (cm) / l (cm)	ki_x / l/s	ki_y / ki_z	(fei)x / (fei)y	(fei)z	fcL_x / fcL_y	fcL_z	σx / σy	τ	factor
Tank Top plane	3211	1854	81.50	4.4	1.2849	4776	6542.1	2692.9	1727.8	246.70	1.90	0.94
	3211	1.950	437.00	5.36	6.027	1394.7		1394.7		12.30		
Inner bottom	2400	1386	81.50	4.4	1.2845	4183	5729.5	2069.5	1305.2	22.10	2.80	0.87
	2400	1.825	438.00	5.37	6.026	1221.3		1221.3		103.20		
T. BHD	2400	1386	81.50	4.4	1.2676	2986	4069.9	1937.1	1272.4	28.90	15.59	1.45
	2400	1.542	489.00	6.00	5.996	860.4		860.4		121.37		
CaseB 50°C												
ID	fy / fyi	fyi_z / tn (cm)	s (cm) / l (cm)	ki_x / l/s	ki_y / ki_z	(fei)x / (fei)y	(fei)z	fcL_x / fcL_y	fcL_z	σx / σy	τ	factor
Tank Top plane	3211	1854	81.50	4.4	1.2849	4776	6542.1	2692.9	1727.8	92.35	2.91	0.35
	3211	1.950	437.00	5.36	6.027	1394.7		1394.7		5.35		
Inner bottom	2400	1386	81.50	4.4	1.2845	4183	5729.5	2069.5	1305.2	4.29	2.74	0.65
	2400	1.825	438.00	5.37	6.026	1221.3		1221.3		77.39		
T. BHD	2400	1386	81.50	4.4	1.2733	3317	4527.5	1983.2	1283.9	21.09	18.08	0.83
	2400	1.625	470.00	5.77	6.006	959.8		959.8		76.02		
CaseB 80°C												
ID	fy / fyi	fyi_z / tn (cm)	s (cm) / l (cm)	ki_x / l/s	ki_y / ki_z	(fei)x / (fei)y	(fei)z	fcL_x / fcL_y	fcL_z	σx / σy	τ	factor
Tank Top plane	3211	1854	81.50	4.4	1.2849	4776	6542.1	2692.9	1727.8	97.28	2.90	0.38
	3211	1.950	437.00	5.36	6.027	1394.7		1394.7		11.34		
Inner bottom	2400	1386	81.50	4.4	1.2845	4183	5729.5	2069.5	1305.2	36.86	0.71	0.97
	2400	1.825	438.00	5.37	6.026	1221.3		1221.3		114.42		
T. BHD	2400	1386	81.50	4.4	1.2733	3317	4527.5	1983.2	1283.9	26.41	23.03	1.16
	2400	1.625	470.00	5.77	6.006	959.8		959.8		106.63		

4.3 Discussion

Table 8 and 9 shows utilization factors for yield and buckling when mechanical loadings are applied. In this study, since both static and dynamic mechanical loadings are applied, the corresponding utilization factors are marked in Table 8 and 9. In CSR, thermal loadings are not considered and only mechanical loadings (both static and dynamic) are considered. So, it is believed that a certain safety margin by thermal loading was considered in CSR. Although the structure shows stresses beyond yield, it does not mean the failure of the structure. When thermal loadings are included additionally, higher criteria may be considered or mechanical loadings may be adjusted. The level of enhanced criteria should be further discussed among the relevant industries.

Table 8 CSR criteria for stress (Table 9.2.1 of CSR)

SECTION 9 - DESIGN VERIFICATION   COMMON STRUCTURAL RULES FOR OIL TANKER

Table 9.2.1
Maximum Permissible Stresses

Structural component	Yield utilisation factor
Internal structure in tanks	
Plating of all non-tight structural members including transverse web frame structure, wash bulkheads, internal web, horizontal stringers, floors and girders. Face plate of primary support members modelled using plate or rod elements	$\lambda_y \le 1.0$ (load combination S + D) $\lambda_y \le 0.8$ (load combination S)
Structure on tank boundaries	
Plating of deck, sides, inner sides, hopper plate, bilge plate, plane and corrugated cargo tank longitudinal bulkheads. Tight floors, girders and webs.	$\lambda_y \le 0.9$ (load combination S + D) $\lambda_y \le 0.72$ (load combination S)
Plating of inner bottom, bottom, plane transverse bulkheads and corrugated bulkheads.	$\lambda_y \le 0.8$ (load combination S + D) $\lambda_y \le 0.64$ (load combination S)

(S : static loading, D : dynamic loading)

Table 9 CSR criteria for buckling (Table 9.2.2 of CSR)

SECTION 9 - DESIGN VERIFICATION   COMMON STRUCTURAL RULES FOR OIL TANKERS

Table 9.2.2
Maximum Permissible Utilisation Factor Against Buckling

Structural component	Buckling utilisation factor
Plate and stiffened panels (3)	$\eta \le 1.0$ (load combination S + D) $\eta \le 0.8$ (load combination S)
Web plate in way of openings	$\eta \le 1.0$ (load combination S + D) $\eta \le 0.8$ (load combination S)
Pillar buckling of cross tie structure	$\eta \le 0.75$ (load combination S + D) $\eta \le 0.65$ (load combination S)
Corrugated bulkheads - flange buckling - column buckling	$\eta \le 0.9$ (load combination S + D) $\eta \le 0.72$ (load combination S)
Where: η utilisation factor against buckling calculated in accordance with *Appendix D/5* and *Appendix B/2.7.3*. Also see *Section 10/3.4.1* for web plate in way of openings and *Section 10/3.5.1* for cross tie structure	

(S : static loading, D : dynamic loading)

5 Conclusion

Currently, tankers are designed under CSR. Since the deformation load due to thermal loading up to 80 ^{o}C of cargo temperature is not covered by CSR and so far there have been few studies on the design of cargo hold considering thermal loading. In this study, the strength analysis of a cargo hold is performed by considering thermal loading only, mechanical loading only, and the combination of thermal and mechanical loading through finite element analysis.

Through the analyses, it is seen that stress distribution due to the thermal loading only is unrealistic and stress from the combined loading is not increased dramatically from that of the mechanical loading. Also the effect of thermal loading on the stress distribution and buckling is observed. Since cargo hold is designed under CSR loading and corresponding criteria, when the thermal loading is included additionally, higher criterion may need to be considered. The necessity of considering thermal loading and the level of enhanced criteria should be further studied.

Reference

[1] ABS RULES FOR BUILDING AND CLASSING, STEEL VESSELS 2010. PART 5A SPECIFIC VESSEL TYPES (CHAPTER 1), Common Structural Rules for Double Hull Oil Tankers.

[2] Lee, S.W. Choi, J.H. Kim, M.S. Kim, M.S. Lee, Y.M. & Kim, K.S., 2005. Structural Strength and Fatigue Strength Assessment for Fore/Aft Cargo Hold of 60m Beam VLCC. *Special Issue of the Society of Naval Architect of Korea*, pp.84-89.

[3] Na, S.S. Yum, J.S. & Kim, Y.S., 2010. The Structural Design of a Large Oil Tanker based on the CSR by Considering the Web Arrangement and Material Property. *Journal of the Society of Naval Architects of Korea*, 47(4), pp.598-605.

[4] Kim, S.I. Kim, Y.N. & Kim, G.R., 2007. Consideration of AFRAMAX TANKER Applied Common Structural Rules. *Special Issue of the Society of Naval Architect of Korea*, pp.99-106.

[5] Na, S.S. & Jeon, H.G., 2008. Optimal Structural Design of Mid-ship Section of D/H Tankers Based on Common Structural Rules. *Journal of the Society of Naval Architects of Korea*, 45(2), pp.151-156.

[6] Jo, Y.C. Lee, J.C. Lee, S.B. Shin, S.K. & Jang, C.D., 2011. Optimal Design for Longitudinal Strength Members of Double Hull Tankers with Central Long'l Bulkhead considering Bucking Thickness Required of Plate Panels based on Common Structural Rules. *Special Issue of the Society of Naval Architect of Korea*, pp.117-126.

[7] So, H.Y. Lee, K.H. Shin, S.K. Choi, Y.D. & Leem, H.K., 2007. Structural Analysis of MR. Sized Oil Tanker Applied Common Structure Rule. *Special Issue of the Society of Naval Architect of Korea*, pp.26-31.

[8] MSC. Nastran 2010. Linear Static Analysis User's Guide.